CHAPTER 4

Atmospheric CO_2 fluctuations during the last Millennium reconstructed by stomatal frequency analysis of *Tsuga heterophylla* needles

The inverse relation between atmospheric CO_2 concentrations and stomatal numbers on *Tsuga heterophylla* needles was applied to reconstruct paleo-atmospheric CO_2 concentrations over the period 800-2000 AD from fossil *T. heterophylla* needles in a lake sediment core from Mount Rainier, Washington, USA. The stomatal frequency record revealed significant century-scale fluctuations, with prominent minima in CO_2 of about 260 ppmv present around 860 AD and 1150 AD, and smaller minima of 275-280 ppmv occurring around 1600 and 1800 AD. In between, CO_2 maxima of 300 ppmv around 1000 AD, 320 ppmv around 1300 AD, and 300 ppmv around 1700 AD are recorded. These features occur in harmony with global terrestrial temperature changes, as well as oceanic surface temperature fluctuations in the North Atlantic. The results obtained in this study reinforce the notion of a continuous coupling of CO_2 and climate during the Holocene, as previously suggested by stomatal frequency records from the last Deglaciation and Early Holocene.

INTRODUCTION

The notion of tightly co-varying atmospheric CO_2 levels and climate is reinforced by the prediction in climate models of both a strong rise in global mean temperature as a result of the continuous injection of anthropogenically produced CO_2 in the atmosphere ((1-7ºC; IPCC, 2001), as well as significant feedback effects of these CO_2 induced climate changes on the carbon exchange between oceanic, atmospheric and terrestrial reservoirs (Joos et al., 1999; Yi et al., 2001; Plattner et al., 2001; Dore et al., 2003).

Late Quaternary atmospheric CO_2 concentrations (mixing ratios) and isotopic temperature records reconstructed from Antarctic ice-cores show parallel variations on glacial-interglacial time scales (Raynaud et al., 1993; Petit et al., 1999). On millennial time scales, a similar co-variation has been recognized during the glacial periods (Stauffer et al., 1998; Fischer et al., 1999; Indermühle et al., 2000). In marked contrast, however, ice-core data suggest that during the interglacials, like the Holocene, global temperature variations and atmospheric CO_2 concentrations are decoupled. Long-term global temperature trends, such as the warm Holocene Hypsithermal and the successive Subatlantic cooling, have not been recognized in the Antarctic CO_2 records, which have their lowest values in the early Holocene around 8000 BP and then rise gradually from 260 ppmv to pre-industrial 280 ppmv (Indermühle et al., 1999a; Flückiger et al., 2002).

On centennial time scales, no significant ice-derived CO_2 fluctuations occur contemporaneously with well-documented cooling events such as the Younger Dryas, Preboreal Oscillation, and the 8.2 kyr BP event. Intriguingly, however, several Antarctic ice core records of the last millennium do show CO_2 changes of 5–20 ppmv that are broadly concurrent with the Medieval Climatic Optimum and Little Ice Age (Barnola et al., 1995; Etheridge et al., 1996; Indermühle et al., 1999a). Although these records could indicate a coupling between temperature shifts and atmospheric CO_2, data from different coring localities are not in agreement with respect to timing and magnitude of the CO_2 changes (Siegenthaler et al., 1988; Barnola et al., 1995; Etheridge et al., 1996; Indermühle et al, 1999a).

An alternative proxy for atmospheric CO_2 concentration is provided by means of stomatal frequency analysis, where the inverse relation between the number of gas pores on plant leaves and ambient CO_2 enables the reconstruction of past CO_2 levels (e.g. Woodward,1987; Kürschner et al, 1996; Wagner et al., 1996; Royer, 2001; Royer et al., 2001). Stomatal records show a much more dynamic CO_2 evolution during the last Deglaciation and Holocene than the ice-core measurements. Reconstructed centennial-scale CO_2 fluctuations in the order of 20-80 ppmv can be related to cooling events such as the Younger Dryas (Beerling et al., 1995; McElwain et al, 2002; Rundgren and Björck, 2003), Preboreal oscillation (McElwain et al., 2002; Wagner et al., 1999a), the 8.2 kyr event (Wagner et al., 2002) and the Little Ice Age (Rundgren and Beerling, 1999). These reconstructions contradict the concept of an Early-Holocene decoupling of CO_2 and temperature, postulated on the basis of ice-core records.

In the stomata-based reconstructions, and in some ice-core records, CO_2 fluctuations occur approximately synchronous with Holocene temperature changes. There may be a slight time-lag at the end of the Younger Dryas (McElwain et al., 2002), but insufficient temporal resolution and chronological uncertainty of the stomatal data and ice-core measurements has hampered accurate determination of the exact phase-relation between CO_2 and climate on centennial time scales.

In addition to leaves of angiosperm tree species, needles of conifers are increasingly used for detecting and quantifying past CO_2 changes (Van de Water et al., 1994; Royer et al., 2001; McElwain et al., 2002). In the present study we document the stomatal frequency analysis of a high-resolution record of fossil *Tsuga heterophylla* needles from North America. Spanning the period between 800 AD and 2000 AD, the results are used to ascertain whether global or extra-regional temperature trends for the last Millennium, inferred from both marine and terrestrial proxy records, are indeed associated with a dynamic atmospheric CO_2 regime.

MATERIAL AND METHODS

A record of fossil needles of the conifer *Tsuga heterophylla* over the past 1200 years was obtained from the upper 44 cm of a 91 cm sediment core, drilled in Jay Bath, a shallow pond (about 1.20 m water depth) on the southern flank of Mount Rainier (Washington, USA; 46º46' N 121º46' W; Fig. 4.1). These sediments contain rich and diversified needle assemblages (Dunwiddie, 1986). The needles can be identified at a species level. Relative-fre-

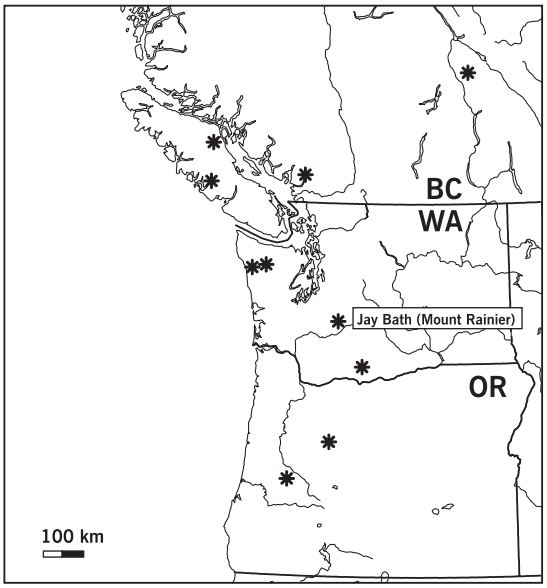

Figure 4.1: Source localities of the *Tsuga heterophylla* needles used in the training set and the location of Jay Bath (Mount Rainier National Park). BC = British Columbia (Canada), WA = Washington (USA) and OR = Oregon (USA).

quency patterns indicate that the needle record of the studied interval originates from a stable, late-successional forest dominated by *T. mertensiana*, *T. heterophylla* and *Abies amabilis.*

The core was cut into 1 cm thick sediment samples, which were sieved on a 250µm mesh sieve. *T. heterophylla* needles were identified and stored in ethanol. Needles for stomatal analysis were bleached with a 4% natriumhypochloride solution to remove the mesophyll. The remaining cuticle was then stained with safranin and mounted in glycerin jelly on a microscopic slide. Computer-aided measuring of epidermal cell parameters on needle cuticles of *T. heterophylla* was performed on a Leica Quantimet 500C/500+ Image Analysis system (Wetzlar, Germany).

In conifer needles, the number of stomata per mm needle length (TSDL) is the parameter most sensitive to changes in CO_2 concentrations (Chapter 2). The response rate of *T. heterophylla* needles to the CO_2 increase over the last century was used to quantify late-Holocene TSDL-based CO_2 changes (Fig. 4.2). All needles incorporated in the training set originate from the Pacific Northwest region (Fig. 4.1). Because of large altitudinal differences between the sites, CO_2 levels were expressed as partial pressure instead of mixing ratios: pCO_2 (Pa) = CO_2 mixing ratio (ppmv) × barometric air pressure P_B (Pa). Barometric air pressure is estimated according to Jones (1992): $P_B = 101.325/e^{[(z/29.3)/T]}$ where z is altitude above sea level and T air temperature in K (estimated from mean annual temperature at the closest weather station, corrected by a temperature lapse rate appropriate for the region in case of significant altitudinal difference between site and station).

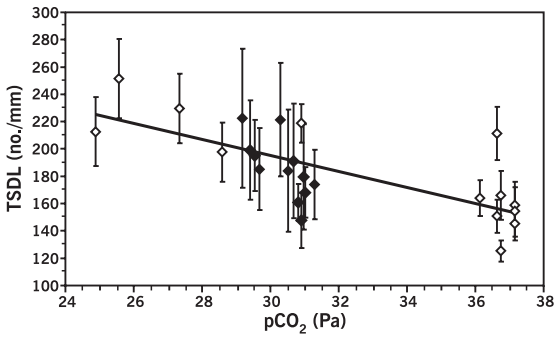

Figure 4.2: Response of stomatal parameters of Tsuga heterophylla to a pCO_2 increase from 24 to 38 Pa. CO_2 partial pressure was calculated as: CO_2 mixing ratio (ppmv) × total barometric pressure P_B (Pa). Barometric air pressure is estimated according to Jones (1992): $P_B = 101.325/e^{[(z/29.3)/T]}$ where z is altitude above sea level and T air temperature in K (estimated from mean annual temperature at the closest weather station, corrected by a temperature lapse rate appropriate for the region in case of significant altitudinal difference between site and station). CO_2 mixing ratios of 290–315 ppmv were derived from shallow Antarctic ice cores (http://cdiac.esd.ornl.gov/trends/co2/siple.htm; Neftel et al., 1985), mixing ratios of 315–368 ppmv are annual means from Mauna Loa monitoring (http://cdiac.esd.ornl.gov/ndps/ndp001.html). Black diamonds represent subfossil and modern needles from Jay Bath (Mount Rainier, WA), open diamonds modern and herbarium needles from other localities. Error bars indicate ± 1 SE. Solid lines indicate best fit in classical regression analysis. TSDL: true stomatal density per mm needle length (TSDL = $-5.8581 \times pCO_2 + 371.14$; $r^2 = 0.5124$; $P < 0.001$).

The stomatal frequency change in the training set is not attributable to changes in local precipitation or temperature (Chapter 2), or affected by difference in age between the needles (Chapter 3). The stomatal frequency response of plants to CO_2 is nonlinear and can best be described by a sigmoid function with upper and lower response limits, because the number of stomata on a leaf can neither be zero nor infinite (Kürschner et al., 1997). *T. heterophylla* apparently does not approach its response limits in the interval between 290 and 370 ppmv, as a linear regression produced a much better fit than non-linear models. Reconstructed CO_2 values were calculated using a classical linear regression, which allows a better performance at the extremes and with slight extrapolation than inverse linear regression (Osborne, 1991; Birks, 1995).

Reconstructed atmospheric CO_2 levels for the last millennium are expressed as mixing ratios rather than the reconstructed partial pressure to allow quantitative comparison with other CO_2 records. Mixing ratios were calculated by dividing the partial pressure by the air pressure at the site studied (1311 m altitude), calculated using the equation of Jones (1992). In this equation modern mean annual temperatures were used, because paleo-temperatures are not known over the whole period since 800 AD. However, temperature at the site has not varied more than approximately 1 ºC between 1500 AD and today (Graumlich and Brubaker, 1986), which would account for a negligible additional uncertainty in reconstructed CO_2 mixing ratio of not more than 0.15 ppmv.

Age-depth relations for the sediment core studied were determined by fitting a 4th order polynomial through a series of five AMS ^{14}C chronologies (calibrated using OxCal 3.8 [Bronk-Ramsey, 1995] and INTCAL98 calibration data [Stuiver et al., 1998]) and one tephra layer at 21 cm from the 1481 Mt. St. Helens eruption (dated by dendrochronology; Yamaguchi, 1983; Mullineaux, 1996). In this way a mean sedimentation rate of one cm per 27 years was obtained for the core (Fig. 4.3).

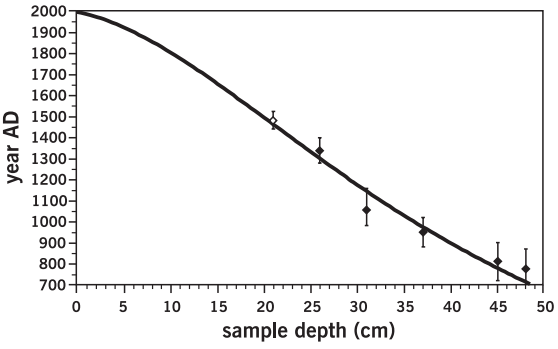

Figure 4.3: Age-depth diagram for Jay Bath core. White diamond represents tephra layer from 1481 Mt. St. Helens eruption (Yamaguchi, 1983; Mullineaux, 1996). Black diamonds represent ^{14}C AMS dates converted to calendar ages using Oxcal 3.8 . Black line shows 4th order polynomial [AGE = −0.00020094 × (DEPTH)^4+ 0.02951 × (DEPTH)^3 − 1.33288 × (DEPTH)^2 − 8.71619 × (DEPTH) +2000.22] providing best fit (r^2 = 0.9977). Error bars indicate 2 sigma (95.4%) probability ranges.

RESULTS

The reconstructed atmospheric CO_2 mixing ratios at Jay Bath since 800 AD are presented in figure 4.4. Pre-industrial CO_2 values fluctuate around a long-term average of 280-290 ppmv culminating in a sharp rise in CO_2 after 1850 AD from 280 ppmv to 370 ppmv. The CO_2 record is characterized by high-frequency variability. Focussing on centennial-scale changes (the 3 point moving average), prominent minima in CO_2 of about 260 ppmv are present around 860 AD and 1150 AD, and smaller minima of 275-280 ppmv occur around 1600 AD and 1800 AD. In between, CO_2 maxima of 300 ppmv around 1000 AD, 320 ppmv around 1300 AD, and 300 ppmv around 1700 AD are recorded.

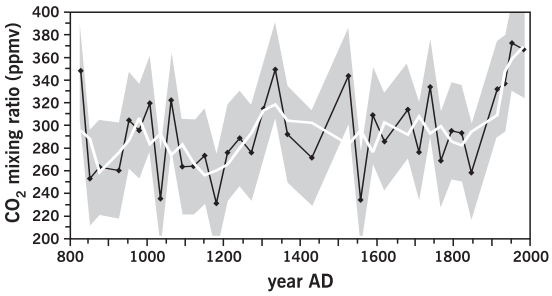

Figure 4.4: Reconstructed CO_2 mixing ratios based on stomatal frequency counts on *Tsuga heterophylla* needles for the time period from 800 AD to 2000 AD. Black line are the means of 3–5 needles per sample, thick white line represents a 3 point moving average. Grey area shows confidence interval of ± 1 RMSE.

DISCUSSION

The sharp rise in the stomata-based CO_2 curve (Fig. 4.5A) after 1850 AD corresponds excellently to the industrial CO_2 increase apparent in instrumental records (Keeling and Whorf, 2002) and shallow ice-cores (Neftel et al., 1985). This correspondence corroborates the reliability of the reconstruction. Mean pre-industrial CO_2 values are simular to those measured in Antarctic ice-cores (Etheridge et al., 1996; Indermühle, 1999a). However, with prominent maxima centred around 1000 AD, 1300 AD, and 1700 AD and minima around 860 AD, 1150 AD, 1600 AD, and 1800 AD, the centennial-scale CO_2 variability during the last millennium is much more pronounced in the stomata-based record than in ice-core data. In the Law Dome ice core these reconstructed fluctuations have not been detected (Etheridge et

al., 1996). On the other hand, CO_2 records from ice-cores D47 and D57 from Adelie Land (Antarctica) exhibit a rapid increase (of 15 ppmv) during the 13th century AD (Barnola et al., 1995). The discrepancies between the different ice-core and stomatal records may partly be explained by varying age distributions of the air in the bubbles due to the enclosure time in the firn-ice transition zone, which depends on local temperatures and accumulation rates. In different ice cores, this effect creates a site-specific attenuation of the signal as well as a difference in age between the air and surrounding ice, hampering the construction of well-constrained time-scales (Schwander et al., 1996; Spahni, et al., 2003). Other potential factors that may create dissimilarities between the records include the application of different extraction methods for CO_2, and post-depositional physicochemical reactions in the ice that can increase as well as decrease the CO_2 concentration in air bubbles (Anklin et al., 1995; Stauffer and Tschumi 2000).

Terrestrial climate changes of the last Millennium conventionally related to the Medieval Warm Period and the Little Ice Age occurred at different times in different parts of the world. Regional cooling trends were often interrupted by periods of relative warmth. It is not attempted, therefore, to correlate reconstructed global CO_2 fluctuations with these regional events. CO_2-temperature correlations on a global or extra-regional scale are illustrated in figure. 4.5.

A comparison of the stomata-based CO_2 reconstruction to a multi-proxy global mean temperature reconstruction (Mann and Jones, 2003) reveals some striking correlations, most remarkably so in the timing of the warm periods and the CO_2 maxima around 950 AD and 1300 AD (Fig. 4.5B). The overall picture suggests a clear co-variation between CO_2 and global temperature. However, detailed matching of the records is hampered by the fact that the Southern Hemisphere contribution to the global mean temperature estimation is based on limited proxy data, as well as the uncertainties in the chronology of the CO_2 record (on the scale of several decades).

To understand cause and effect in the CO_2-temperature coupling, appropriate regional climate records were selected for comparison with the reconstructed CO_2. The timing of CO_2 maxima and minima in the stomata-based record is synchronous (within uncertainty limits) to changes in North Atlantic Ocean sea surface temperature as recorded offshore Mid-Atlantic USA (Cronin et al., 2003; Fig. 4.5C) as well as offshore West Africa (DeMenocal et al., 2000; Fig. 4.5D). The observed synchroneity suggests that the North Atlantic ocean could very well serve as source and sink at the time of centennial-scale atmospheric CO_2 variations. Exchange of CO_2 between atmosphere and ocean is highly dependent on physicochemical factors affecting the solubility of CO_2 in the ocean surface waters such as alkalinity, dissolved inorganic carbon (DIC) content, salinity and temperature (Takahashi et al., 1993; Raven and Falkowski, 1999; Plattner et al., 2001). Because higher temperature induces lower CO_2 solubility, SST decrease would draw down CO_2 from the atmosphere into the surface waters, resulting in lower atmospheric CO_2 levels. Oceanic carbon cycle models incorporate a temperature factor of about 4% change in oceanic pCO_2 per degree tempera-

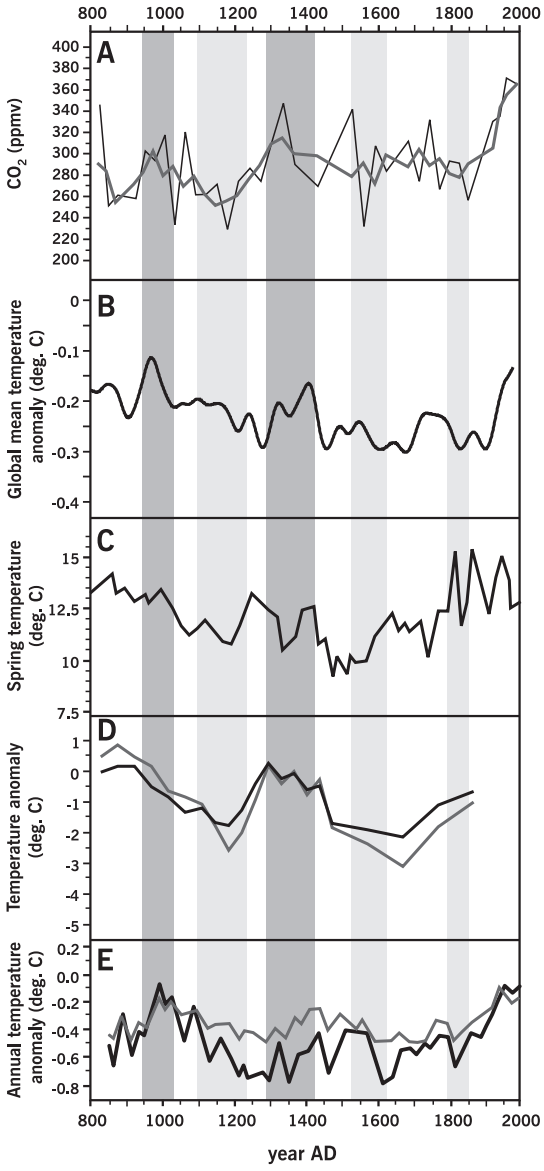

Figure 4.5: Comparison between reconstructed CO_2 mixing ratios and Northern Hemisphere climate records. **A**: CO_2 mixing ratios from stomatal counts on *Tsuga heterophylla* needles from Jay Bath. Thin black line are means of 3–5 needles per sample depth, thick grey line 3 point moving average to emphasize centennial scale trends. **B**: Global mean temperature anomaly (45 year running average) from multi-proxy records based on 1961–1990 reference period (Mann and Jones, 2003). **C**: Sea surface temperatures of Chesapeake Bay (Mid Atlantic USA) reconstructed from Mg/Ca ratios of ostracods (Cronin et al., 2003). **D**: Sea surface temperature anomalies offshore West Africa as reconstructed from foraminiferal assemblages (DeMenocal et al., 2000). Black line are cold season anomalies, grey line warm season anomalies **E**: Summer temperature anomalies in tree ring records from the Northern hemisphere. (Uppermost) grey line from Briffa et al. (2000); (lowermost) black line from Esper et al. (2002). Dark grey shading indicates periods of relatively high CO_2 mixing ratios, light grey shading periods of relatively low CO_2 mixing ratios (panel A).

ture change (equivalent to 11.2 ppmv at a starting level of 280 ppmv; Plattner et al., 2001). For example, a modelled cooling of 2.7 ºC in the Atlantic Ocean (north of 20ºN latitude) during the Younger Dryas produced a local atmospheric pCO_2 decrease of 2.7 Pa (equivalent to 27 ppmv at sea level; Takahashi et al., 1993; Marchal et al., 1999). The SST fluctuations over the last Millennium at the two sites on opposite sides of the Atlantic ocean are of

a similar magnitude (2-3 ºC; Fig. 4.5). Provided that SST at these sites reflects SST changes in the whole North Atlantic, temperature-driven changes in CO_2 flux between ocean surface waters and atmosphere may be invoked as a plausible mechanism to explain at least a substantial part of the reconstructed CO_2 variations over the last Millennium. Additional potential oceanic sources of CO_2 comprise climate-induced changes in salinity, carbonate chemistry (DIC and alkalinity levels), circulation, and marine biological productivity in the Atlantic or the other ocean basins (Siegenthaler and Wenk, 1984; Sarmiento and Orr, 1991; Marchal et al., 1998; Plattner et al., 2001).

The reconstructed CO_2 minima and maxima also show remarkable similarities to Northern Hemisphere temperature trends based on extra-tropical tree-ring records (Briffa, 2000; Esper et al., 2002). A link between CO_2 and terrestrial temperature would be most prominent in Northern Hemisphere records because models of the spatial distribution of a future temperature rise due to anthropogenic CO_2 production indicate that the greatest warming is expected to occur at high latitudes on the Northern Hemisphere continents (IPCC 2001). Models of evolution of CO_2 and Northern Hemisphere temperature in response to changes in radiative forcing over the last Millennium show that temperature changes in the order of magnitude as indicated by the tree-ring record of Esper et al. (2002) are associated with CO_2 changes of at least 20 ppmv (Gerber et al., 2003). Such changes are outside the range of CO_2 variability in ice-cores but compatible with the stomata-based record.

The minimum in the CO_2 record at 1150 AD and the maximum around 1400 AD seem to correspond to terrestrial temperature changes that occur 50-100 years later. However, any exact determination of leads and lags between CO_2 and temperature is impeded by the lower resolution and lower chronological accuracy of the stomata-based reconstruction in comparison to the tree-ring temperature records.

CONCLUSIONS

The centennial-scale variability in atmospheric CO_2 concentration linked to documented global and regional temperature change since 800 AD, recognized in this study, corroborates continuous coupling of CO_2 and climate during the Holocene. For the first time, CO_2 changes inferred from stomatal frequency analysis, have been related to coeval variation in Atlantic sea surface temperatures, providing evidence that CO_2 fluctuations over the last Millennium at least partly originated from temperature-driven changes in CO_2 flux between ocean surface waters and atmosphere. Because CO_2 variation also shows similarities with terrestrial temperature trends in Northern Hemisphere regions most sensitive to global warming, it may be speculated that in the last Millennium CO_2 could have served as a forcing factor for terrestrial temperature.